We would like to thank the reviewers for carefully reading the manuscript and their comments for improving the quality of this paper. The comments and responses are listed below, and the changes are shown in the marked version of the revised manuscript.

Responses to the **1st reviewer's** comments:

1. **The thickness and dimensions of the part should be reported accurately**

Thank you for the comment. The thickness and dimensions of the part have been added through the following revisions to section 3.2 *Composite lay-up definition*:

"The dimensions of the composite were primarily directed by the surface and the heating unit's dimensions. Each temperature zone is roughly 310 mm × 230 mm to ensure that each zone can be placed centrally on the heating pads while maximizing the substrate surface available. The thickness of the glass fiber laminate varies depending on the glass fiber specimen and the pressure exerted by the vacuum and generally lies between 0.7 to 1.2 mm while the foam sample is 12.7 mm at the thickest in zone A and tapers down evenly to 0 in zone B."

2. **All the figures must be described accurately in text. Especially in the results section, figures must be critically commented rather then only reported.**

Thank you for the comments. We have revised the manuscript to provide descriptions and detailed comments to all figures.

3. **Cure kinetics parameters and all the material properties measured should be reported. Anyone should be able to replicate the work presented.**

As suggested, these parameters and material properties are incorporated in Table 1 as shown below. These parameters are sufficient for anyone who has an interest in replicating this work. Note that the values of the pre-exponential coefficient and the activation energy are functions of the degree of cure and are shown in Figures 1a and b.

Material	**Model parameters**	**Value**	**Source of data**
Epoxy resin	Density	1150 kg/m^3	Material datasheet
	Coefficient of thermal conductivity	0.35 W/m.K	
	Newtonian viscosity	0.28 N.s/m^2	Material datasheet
	Specific heat	2500 J/kg.K	DSC measurements
	Enthalpy	450000 J/kg	DSC measurements
	Pre-exponential coefficient (C) for kinetic cure model	Figure 1 (a)	
	Activation energy/Universal Gas constant (E/R)	Figure 1 (b)	
Glass fiber	Density	2520 kg/m^3	Material Datasheet
	Permeability along primary axis	2×10^{-9} m^2	
	Permeability perpendicular to primary axis	8×10^{-18} m^2	

	Thermal conductivity	0.6 × W/m.K	
	Specific heat	840 J/kg.K	
Foam	Density	60 kg/m^3	Temperature data from thermocouples embedded in the system and RFID sensor tags embedded in the composite
	Thermal conductivity	0.029 W/m.K	

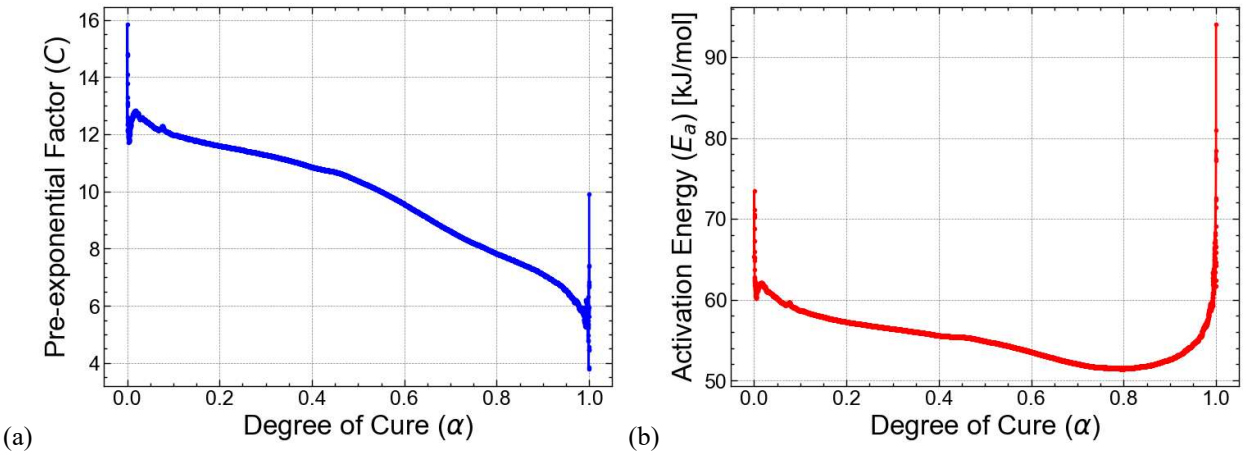

(a) (b)

Figure 1: Calibrated kinetic cure parameters and model validation (a) Pre-exponential factor vs degree of cure, (b) Activation energy vs degree of cure.

4. It is not clear whether the convection boundary condition varies or not and if it does vary how.

The convection boundary varies depending on the lab setting for controlling the temperature. This clarification is in section 3.3 *Multiphysics Simulation* through the following statement:

"Specifically, nodes exposed to ambient air were assigned a convection boundary condition with a heat transfer coefficient ranging from 5.5 to 25 W/m²·K. The value was adjusted based on the laboratory setup and ambient environmental factors including moisture content, air flow conditions, the presence or absence of a cooling fan, thermal blanket, and other natural influences that could not be fully controlled or modeled."

5. The cure profile as a function of temperature and time, applied at the mould side is not reported.

The cure profile is reported in Fig.3, which is obtained based on a trained LSTM neural network and temperature setpoint as input. Fig 3 caption is revised to provide details on the modeling framework.

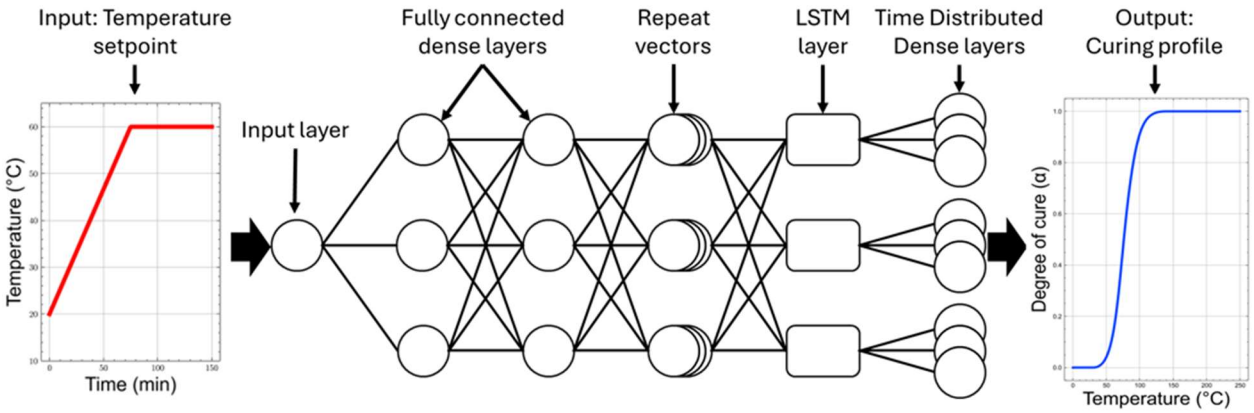

Figure 3: The ML model for the VARIM process. An ML-based prediction model based on trained LSTM neural network is employed. The model takes the temperature setpoint as a scalar input (left) and outputs the curing profile (right). The LSTM node is used in conjecture with fully connected dense layers, repeat vectors, and time-distributed dense layers to realize the prediction.

6. Initial conditions are missing

The initial temperature and pressure are added in the section 3.3 *Multiphysics simulation* though the following statement: "The initial and ambient temperature throughout the process is assumed to be 25 °C and the atmospheric pressure is set to 1 bar."

7. Can you please describe what is intended by conventional method?

Conventional method refers to the industry practice in which the temperature profile is dictated by the slowest curing time cycle in the composite part being made, and that profile is applied across the whole composite structure being made. An explanation of the same is now added to the introduction. "In industrial practice, all zones are heated according to the slowest curing profile to avoid quality issues. In this study, this configuration will be referred to as the "conventional approach," against which the optimized multizone setup is compared."

8. The degree of cure evolution will be determined by the temperature evolution which is different form to to bottom and across the different heating zones, however contour maps or graphs about temperature are not reported

We thank the reviewer for this comment. Configuring heating elements to control temperature through the thickness remains challenging. In practice, such approaches are typically implemented using active cooling (e.g., fans or ice packs) or insulation (e.g., applying a blanket on the surface). These methods are currently under investigation and are not the focus of this manuscript.

In this work, we instead focus on a multi-zone heating element setup that closely resembles configurations used in manufacturing. Additionally, we have not identified any sensors capable of reliably providing through-thickness temperature measurements.

9. Additional experimental work needs to be performed to assess the benefits achieved, four compressive tests is too little and more need to be done to have some statisitcs, I would suggest to focus on other matrix dominated properties as well.

Thank you for your suggestion. Given that bending loads are typical in wind blade structures, we have switched to 4-pt bending tests to determine the mechanical properties. New samples were created using 'conventional' methods and our optimized 'multizone' method and compared. The following section now replaces the mechanical testing and validation section to better present the effects of multizone curing:

"4.3 Experimental validation

The structural performance of the composites manufactured by the two approaches were evaluated to determine the influence of curing strategy subjected to bending loads representative of wind turbine blade structures. Flexural testing was selected because bending is the dominant loading condition experienced by such structures during operation. Four-point bending tests were conducted on foam sandwich and glass fiber laminate specimens from Zones A and C respectively were cut using water jet cutting to characterize their mechanical response under controlled loading conditions. All testing procedures followed the standard method specified by ASTM International. The specimens in their setup are shown in Fig 10.

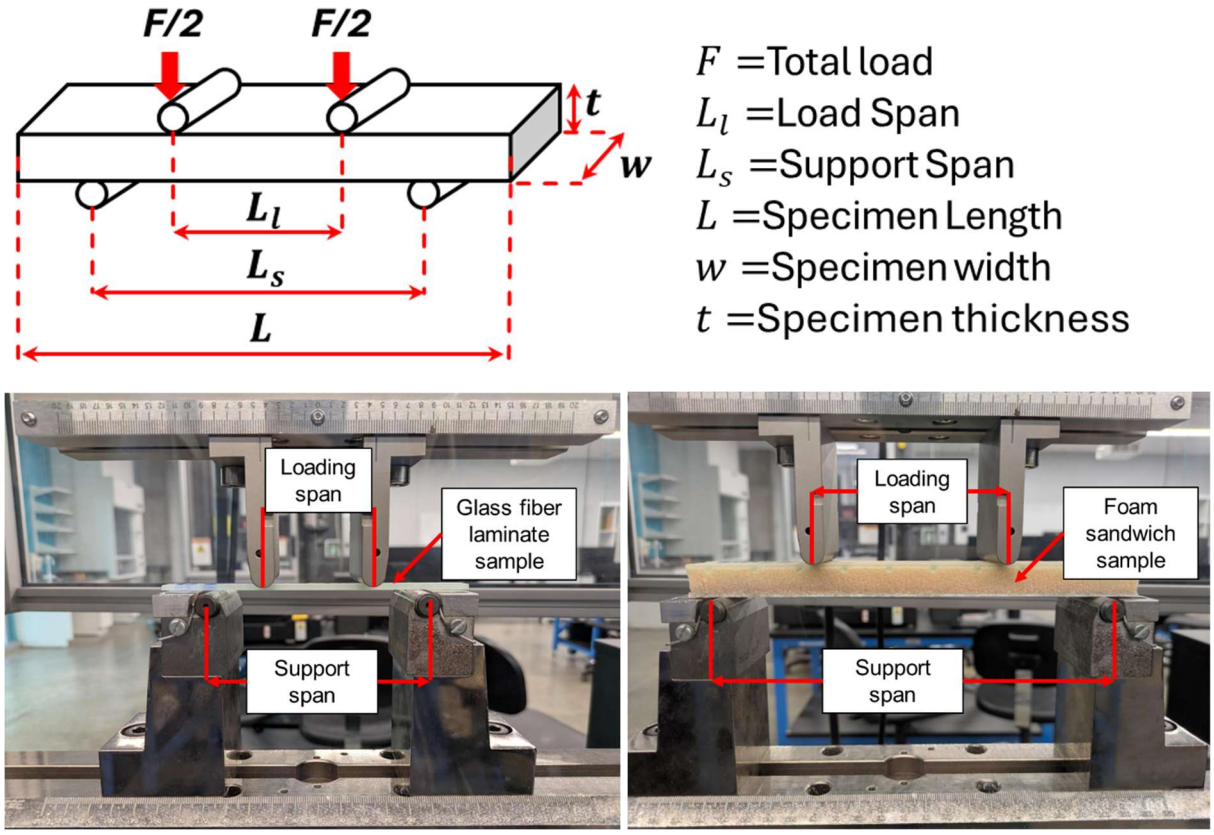

Figure 10: Schematic of the 4-point bending setup (Top). Test performed on glass fiber laminate (Bottom left) and foam sandwich (Bottom right) showing the loading and support spans to ensure pure bending.

The foam sandwich composites from Zone A were in accordance with ASTM standard D7249 (D30 Committee, ASTM International, 2020). The specimens were approximately 14.7 mm thick, 32.8 mm wide, and a support span of 176.4 mm with 20% length overhand on both sides. 4 such samples were cut from each specimen. The load span was half of the support span at 88.2 mm.

For glass fiber laminates from Zone C, 6 samples from conventional and multizone procedures each were cut. The specimen were approximately 12.8 mm wide, 2.3 mm thick, and 140 mm long samples were cut and tested in accordance with ASTM D7264 (D30 Committee, ASTM International, 2021) test method. A support span of 40:1 was chosen, i.e., 92 mm, to ensure failure due to pure bending and to observe compression on top laminate layers and tension in the bottom layers and with load span being half of the support span. The strain rate was determined using the ASTM standard D6272 (D20 Committee, ASTM International, 2017) formula:

$$R = \frac{0.167ZL^2}{d} \tag{13}$$

where R is the rate of crosshead displacement in mm/min, L is the support span in mm, d is the depth of the beam in mm and Z is the rate of straining of the outer fibers which was kept at a minimum value of 0.01 mm/mm.

The flexure stiffness for both the specimens was calculated using equation (14) between strain values of 0.001 and 0.003 as specified by the ASTM standards.

$$E = \frac{\Delta\sigma}{\Delta\epsilon} \tag{14}$$

E = flexural chord modulus of elasticity in MPa, $\Delta\sigma$ = difference in flexural stress between the two selected strain points in MPa, and $\Delta\varepsilon$ = difference between the two selected strain points.

Similarly, the formula for flexural strength is defined in equation (15)

$$\sigma = \frac{3PL}{4bh^2} \tag{15}$$

where: σ = stress at the outer surface in the load span region in MPa, P = applied force in N, L = support span in mm, b = width of beam in mm, and h = thickness of beam in mm.

The average value with errors for the conventional and multizone setup is shown in Fig 10. Table 2 presents the individual values of each specimen.

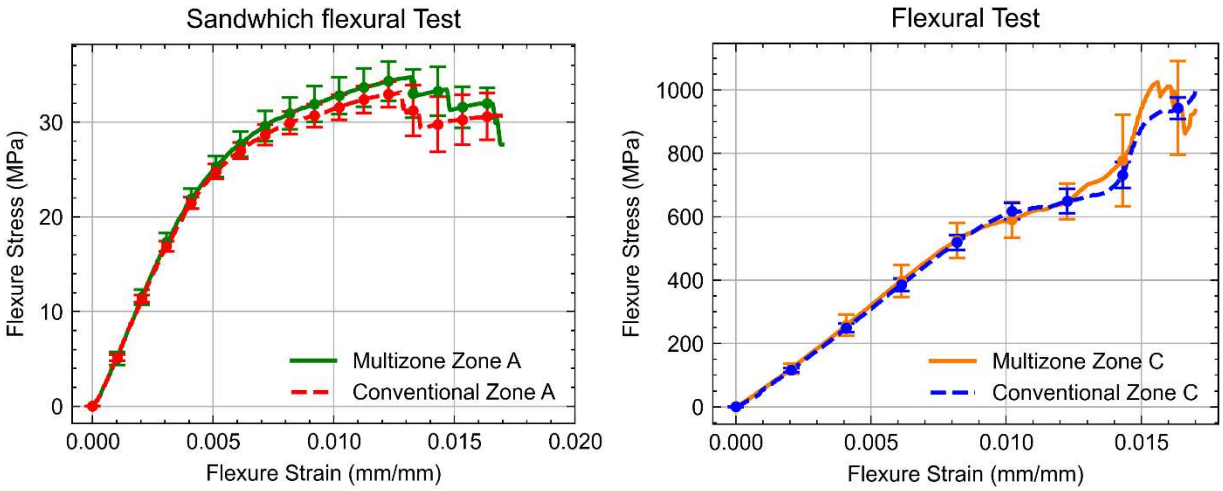

Figure 11: Average and standard deviation of stress vs strain curves for foam sandwich composites (Left) and glass fiber laminates (Right).

	Flexural Stiffness (MPa)	**Percentage difference**	**Flexural strength (MPa)**	**Percentage difference**
Foam sandwich composite using conventional method	5,693.85 ± 146.77	4.68 %	179.66 ± 72.02	4.68 %
Foam sandwich composite using multizone method	5,960.60 ± 189.97		188.06 ± 75.79	
Glass fiber composite using conventional method	61,747.16 ± 3,476.47	4.97 %	1246.32 ± 4.20	3.21 %

Glass fiber composite using multizone method	64,815.55 ± 9,213.66		1286.32 ± 4.51	

Table 2: A summary of flexural modulus and flexural strength calculated from mechanical testing

The flexural test results indicate a consistent 4–5% increase in both the modulus of elasticity and flexural strength for specimens produced using the optimized multizone curing strategy. This improvement suggests that the multizone approach not only matches but also exceeds the mechanical performance achieved through the conventional uniform-temperature process. The enhancement is likely attributable to the reduced thermal gradients and improved cure uniformity associated with multizone temperature control, which mitigates defect formation and promotes more homogeneous material properties. As a result, the composites produced under optimized conditions exhibit greater resistance to bending-induced stresses, delaying the onset of failure and improving overall structural reliability."

10. A sensisitvity analysis between cure non-uniformity and decrease in mechanical performacne should be performed.

Thank you for the suggestion. This analysis would require extensive efforts in designing experiments to achieve different non-uniformity and validate the mechanical properties, which is beyond the scope of this work. In this study our objective is to find the optimum temperature profiles to reduce the curing cycle, minimize the non-uniformity and optimize the mechanical property which can be implemented by industry.

11. The degree of cure and temperature history through thickness is likely to be the one affectiing the matrix dominated properties however the paper is silent about it

Thank you for the comments. As noted in our response to Question 8, active cooling and insulation approaches have been employed in industry practice. However, these implementations remain largely empirical due to the challenges associated with probing the through-thickness cure and temperature distributions. This difficulty is further compounded by the highly heterogeneous and non-uniform structure of the blade cross-section.
The primary focus of this work is to reduce non-uniformity in the in-plane direction, which arises from the large planar dimensions of the blade. While through-thickness non-uniformity may be mitigated using active approaches, a systematic study of such methods has not, to the best of our knowledge, been conducted and remains an area of ongoing investigation.

12. In Figure 7 the process ends after 40000 minutes (660 h), It must be seconds, which would still mean 11 hours. The optimiser should be used to find faster cure cycle.

Thank you for pointing out this error. We have corrected this in Figure 7 (copied below). With this correction, we show that the optimized multizone approach provides faster cure cycle as indicated by the red dashed line shown in the Figure. It was observed that the conventional methods take 631.8 mins to reach saturation while the multizone approach requires 552.8 minutes which amount to roughly 12.5% increase in curing cycle time.

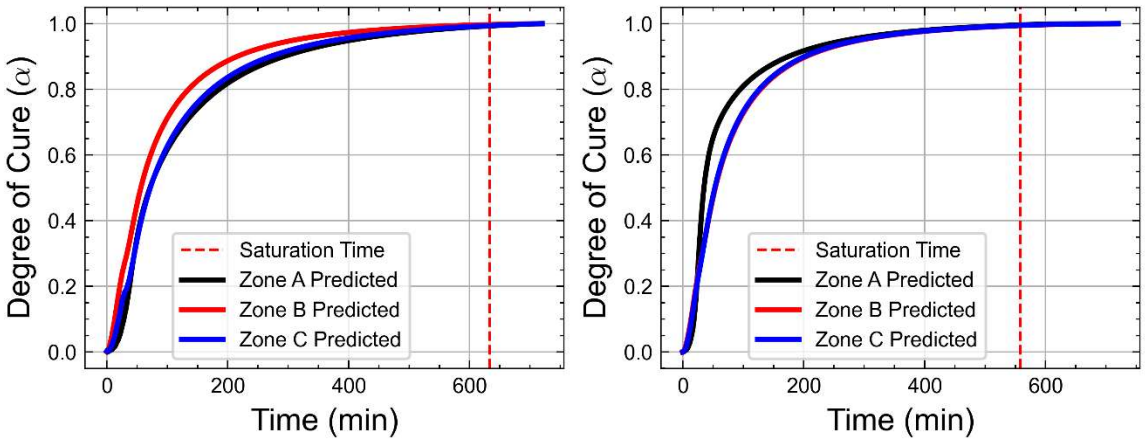

Figure 8: Multiphysics simulations with conventional (Left) and multizone (Right) setups along with degree of cure saturation point showing an improvement in the curing cycle time.

13. In Fig 1, it is not a simulation but a material model therefore the legend should be corrected.

Figure 1 presents the simulated curing response obtained by modeling the resin using a single element. The response is computed by applying the heating rate used in the DSC experiment together with the curing kinetic model parameters. This is not merely a material model evaluation; the simulation also accounts for convective heat transfer with the surrounding air and the exothermic reaction of the 10 g resin sample within the DSC chamber. This clarification has been added to the figure caption.

Figure 1: Calibrated kinetic cure parameters and model validation (a) Pre-exponential factor vs degree of cure, (b) Activation energy vs degree of cure.

14. Celsius symbol is °C whilst Kelvin is K, please correct throughout the paper

All figures were edited to include Celsius as ^{o}C

15. Degree of cure is alpha and not a in Fig 1

Corrections were made.

16. Reference by Maduro is in capital letters and should be corrected

Corrections were made.